JOURNAL OF APPLIED ELECTROCHEMISTRY 7 (1977) 107–112

Hydrodynamic effects on the efficiency of porous flow-through electrodes

B. G. ATEYA, E. A. S. ARAFAT, S. A. KAFAFI

Chemistry Department, Faculty of Science, Cario University, Cairo, Egypt

Received 23 April 1976

Hydrodynamic conditions in porous flow-through electrodes are discussed with special emphasis on radial diffusion effects on the efficiency of reactant conversion. The effect of porosity and tortuosity on the conversion efficiency are also considered. It is shown experimentally that radial diffusion limits the electrode efficiency for $\phi(L) = vr^2/2DL > 0{\cdot}5$ and normal porosity and tortuosity values; $\theta q \simeq 1$. For $\phi(L) < 0{\cdot}5$, the electrode works with 100% efficiency.

A porous flow-through electrode is divided, in the most general case, into three regions: (a) velocity entrance length $h \sim 0{\cdot}2vr^2/\nu$ in which a steady velocity profile is developing; (b) diffusional entrance length $H \simeq vr^2/2D$ for which $\phi(x) = vr^2/2Dx \geqslant 1$; in this region a radial diffusional concentration profile is developing and h is usually much smaller than H; (c) the region where the velocity and concentration profiles are fully developed. Only in region (c) does the electrode operate with 100% efficiency. In regions (a) and (b) radial diffusion limits the electrode efficiency.

1. Introduction

Porous flow-through electrodes are currently attracting much attention in view of their potential industrial applications. Thus, in addition to their obvious uses in fuel cells and in electrosyntheses, such electrode systems have been suggested for the electrochemical removal of copper [1, 2] and antimony [3] and the oxidation of ferrous to ferric ions in industrial waters [4].

This type of electrode offers three major advantages as compared with stationary porous electrodes.

(1) Very high mass transfer rates even at moderate flow speeds; hence concentration limitations can be considerably eliminated;

(2) If the electrode is working at complete reactant conversion, the outflowing solution contains pure product and the electrode acts as a separator between product and unconsumed reactant.

(3) It enables continuous operation as compared with batch processes in stationary systems. With proper optimization, this feature could lead to significant reductions in cost per unit of product.

The maximum limiting current density obtainable from this electrode system i_{L1} in the absence of any rate limitation is:

$$i_{L1} = nFvR_b \qquad (1)$$

where v is the superficial flow speed in cm s^{-1} given by $v = Q/a$ (where Q is the volume flow rate in cm^3 s^{-1} and a is the geometrical cross-sectional area of the electrode), R_b is the inlet concentration of reactant, n is the number of electrons and F is the Faraday. The efficiency of the electrode can be seriously limited by radial diffusion effects, i.e. the experimental limiting current becomes less than that which is given by Equation 1, hence the electrolyte leaves the electrode at the exit face only partly reacted.

It has been recently shown [5, 6] that complete reactant conversion is possible only when the radial diffusion time [7] $\tau = r^2/2D \leqslant$ the residence time (r.t. $= L/v$) of the electrolyte i.e. $r^2/2D \leqslant L/v$ is a necessary condition for complete conversion, i.e. for Equation 1 to be obeyed. The ratio τ/r.t. $= vr^2/2DL = \phi(L)$.

Thus for complete conversion

$$\phi(L) = vr^2/2DL \leqslant 1. \qquad (2)$$

For incomplete conversion

$$\phi(L) > 1.$$

At the limit of very large $\phi(L)$ values, the

system approaches the flow in a tube treated previously by Levich [8], Equation 16. A question then arises concerning the value of $\phi_{\text{lim}}(L)$ and the degree of conversion for intermediate values of $\phi(L)$, i.e. $1 < \phi(L) < \phi_{\text{lim}}^{(L)}$ where $\phi_{\text{lim}}^{(L)}$ is the limiting value beyond which the flow regime given by Levich (Equation 16) is prevailing?

The purpose of this communciation is to present analytical solutions to these questions, and to compare them with experimental results. In addition, the effects of porosity and tortuosity on the conversion efficiency are discussed. The treatment is presented for tubular pores and then modified to account for porosity and tortuosity effects in actual porous electrodes.

2. Model and solution

Firstly, let us consider a tubular pore with fully developed velocity and concentration profiles and negligible entrance effects. These assumptions are commonly adopted in treating porous flow-through electrodes. As will be shown later these assumptions are justified only for low flow rates and electrodes of fine pores [9]. A further objective here is to test the validity of these assumptions and determine the value of $\phi(L)$ below which these assumptions are justified.

For a constant concentration R_w at the pore wall over the electrode length, and by analogy with radial heat transfer in laminar flow [10], the solution is [9]

$$(Nu) = kd/D = 3{\cdot}66 \tag{3}$$

where (Nu) is the Nusselt number, D is the diffusion coefficient in $cm^2\ s^{-1}$, d is the pore diameter in cm and k is the radial mass transfer coefficient in $cm\ s^{-1}$. The radial mass transfer rate per unit area of pore surface is

$$\text{the rate of radial diffusion} = k[R_m(x) - R_w]$$

where $R_m(x)$ is the concentration at the pore centre at x. Clearly, at the limiting current, $R_w = 0$ along the pore length, hence

$$\text{the rate of radial diffusion} = 3{\cdot}66(D/d)R_m(x). \tag{4}$$

Performing a mass balance in the axial direction on a space element dx, Fig. 1, gives

$$di = -nFv\, dR_m(x). \tag{5}$$

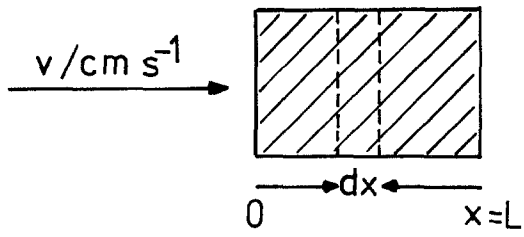

Fig. 1. Geometrical model of a porous flow-through electrode.

Axial diffusion is neglected in this equation. This is justified [11] for $D/Lv < 0{\cdot}01$ i.e. if $L = 1$ cm, $D = 10^{-5}\ cm^2\ s^{-1}$, then axial diffusion is negligible for $v > 0{\cdot}001\ cm\ s^{-1}$. The current di of Equation 5 is supported by radial diffusion to the internal surfaces of the pores in the space element dx, thus

$$di = 3{\cdot}66nF(D/d)R_mA\ dx \tag{6}$$

where A is the peripheral surface area of the porous electrode in $cm^2\ cm^{-3}$. Integration of Equation 5 and using $R_m(0) = R_b$ as a boundary condition gives

$$i(x) = nFv[R_b - R_m(x)]. \tag{7}$$

Combining Equations 6 and 7, rearranging and integrating one obtains

$$dR_m(x)/R_m(x) = -3{\cdot}66(AD/dv)\ dx.$$

This equation is integrated using the boundary condition $x = 0, R_m = R_b$ to give at $x = L$

$$R_m(L) = R_b \exp[-3{\cdot}66(AD/dv)L]. \tag{8}$$

Substituting in Equation 7 gives

$$i_{L2} = nFvR_b\{1 - \exp[-3{\cdot}66(AD/dv)L]\}$$
$$= i_{L1}\{1 - \exp[-3{\cdot}66(AD/dv)L]\}, \tag{9}$$

where i_{L2} is the limiting current in the presence of radial diffusion limitations. Consequently the conversion efficiency f is

$$f = 1 - \exp[-3{\cdot}66(AD/dv)L] \tag{10}$$

where $f = i_{L2}/i_{L1}$. Austin *et al.* [9] obtained this equation and concluded that for electrodes of fine pores the above exponent has a large negative value and f is practically unity.

The peripheral surface area A is related to the mean pore diameter d and the porosity θ by [12]

$$A = 4\theta/d. \quad (11)$$

Substituting in Equation 10 and putting $d = 2r$ gives

$$f = 1 - \exp[-3{\cdot}66D/r^2L/v]. \quad (12)$$

A similar equation has been recently derived by Wroblowa and Razumney [13].

A porous electrode is essentially an isotropic network of highly interlinked pores. Since $v = Q/a$, then the actual velocity of electrolyte inside the pore v_p must depend on the fraction of a available for the electrolyte flow i.e. on the porosity θ; thus $v_p = v/\theta$. It has long been recognized that v_p is several times greater than v; a factor of 4–8 was suggested by Muskat [14]. Furthermore, the actual distance travelled by the electrolyte is qL where q is the tortuosity factor, the value of which is usually between $\sqrt{2}$ and 2 for normal porous solids [15]. Consequently the actual r.t. is given by

$$\text{actual r.t.} = qL/v_p = \theta qL/v$$
$$= \theta qx \text{ (apparent r.t.)}.$$

In order for Equation 12 to correspond to experimental conversion efficiencies in porous electrodes, L/v should be replaced by the ratio of the actual quantities, thus

$$f = 1 - \exp[-1{\cdot}83\theta q/\phi(L)]. \quad (13)$$

By analogy, Equation 9 becomes

$$R_m(x)/R_b = \exp[-1{\cdot}83\theta q/\phi(x)]. \quad (14)$$

Equations 13 and 14 show that as $\phi(x)$ decreases (fast radial diffusion and long residence time) $R_m(x)/R_b$ decreases exponentially whereas f increases, becoming ultimately equal to unity for small $\phi(L)$. Under this condition, the exponential term in Equation 9 is negligible and the equation becomes identical to Equation 1. For the same value of $\phi(L)$, f increases with increasing θ and/or q. This effect of porosity can be explained on the basis of the above discussion. Thus as the porosity increases (constant $\phi(L)$), the actual flow speed inside the pore (at a certain flow rate) decreases; hence f increases. As q increases, the actual path length of the electrolyte inside the electrode increases and so also does the actual residence time; hence f increases.

Fig. 2 shows the dependence of f on both $\phi(L)$ and the product θq. It is seen that a high

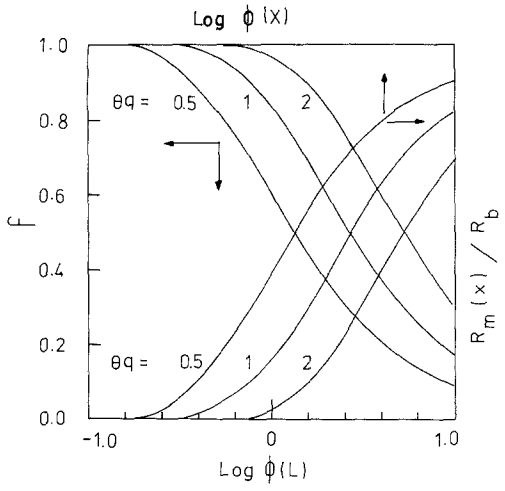

Fig. 2. Effects of $\phi(L)$ on the efficiency and of $\phi(x)$ on the concentration profile in a flow-through electrode.

conversion efficiency is favoured by small $\phi(L)$ or large θq values. This agrees with the above physical reasoning. The figure also shows the variation of the ratio $R_m(x)/R_b$ with $\phi(x)$ and θq. It is seen that as $\phi(x)$ decreases (or θq increases) $R_m(x)/R_b$ decreases, becoming ultimately equal to zero when $f = 1$.

3. Experimental

The flow-through cell used in the measurements is shown schematically in Fig. 3. The polarization at the entrance face η_0 was measured against the reference electrode R_2, whereas that at the exit face η_1 was measured versus R_1. The reference electrodes were Hg/Hg_2SO_4 (in 1 N H_2SO_4). The two counter electrodes offer the option of changing the direction of the current flow with respect to the electrolyte flow. The two contacts to the working electrodes were used to measure the electronic resistance of the packed bed electrode. This was always found to be negligible ($< 0{\cdot}05\ \Omega$). The electrode was positioned vertically and the electrolyte was made to flow in the upward direction under a constant pressure head generated by a simple flow system.

The electrode was made of cylindrical copper particles (0·04 cm diameter by about 0·2 cm length). These particles were uniformly packed and then pressed to ensure good electrical contact. The porosity of the packed bed electrode was calculated

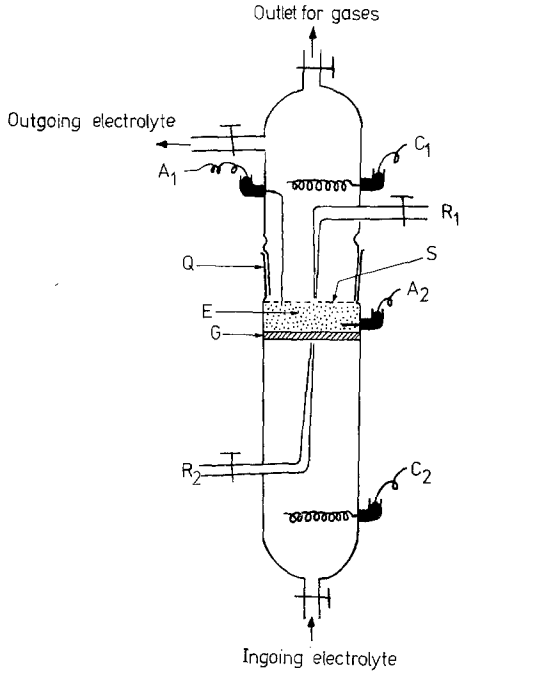

Fig. 3. Flow-through cell.

from the weight of the packed particles and the density of copper. The flow speed was calculated by measuring the volume of the electrolyte flowing during the course of an experiment; $v = Q/a$, where Q is the volume flow rate and a is the geometrical cross-sectional area of the electrode. The diameter of the packed bed was 2 cm and its length was 2·1 cm, hence edge effects can be neglected.

The above cell and flow system were used in performing liquid permeability measurements from which the mean pore diameter and the peripheral surface area of the porous electrode were calculated [11, 12].

The limiting current was measured for the deposition of Cu^{2+} and for the (2-electron) reduction of oxygen, both on the packed bed copper electrode in 1 N H_2SO_4 at room temperature 25 ± 2° C. The solutions were $1{\cdot}8 \times 10^{-4}$ M $CuSO_4$ (de-aerated with prepurified nitrogen) and $3{\cdot}3 \times 10^{-4}$ M dissolved oxygen, both in 1 N H_2SO_4. The concentrations were determined polarographically. The limiting current was determined using a simple steady-state galvanostatic technique. A constant cathodic current was passed and a steady potential reading was soon obtained. Under all flow speeds and concentrations, a well-defined mass transfer limiting current was easily determined from the plot of the current–potential data.

4. Results and discussion

The tortuosity of the packed bed electrode was calculated from the electrolytic resistance of the electrolyte filling its pores. This in turn was calculated by measuring the ohmic potential drop between the two reference electrodes, while a constant d.c. current was flowing between the two counter electrodes. This resistance [12] equals $R_{\mathrm{eff}} = R_{\mathrm{free}} q/\theta$, where R_{free} is the resistance of the same electrolyte column without copper packing. Hence by knowing R_{free} and θ, q can be calculated. The value of q so obtained was about 1·75 which is well within the range of accepted values [15].

The liquid permeability of the electrode was calculated from the pressure-flow rate data and then used to calculate the mean pore diameter of the electrode [11, 12]. The equivalent pore radius was found to be 67 μm. In calculating the value of $\phi(L)$, the diffusion coefficient of Cu^{2+} was taken from reference [16] as $7{\cdot}5 \times 10^{-6}$ cm^2 s^{-1} for $1{\cdot}8 \times 10^{-4}$ M $CuSO_4$ at 25° C.

Fig. 4 shows a comparison of experimental

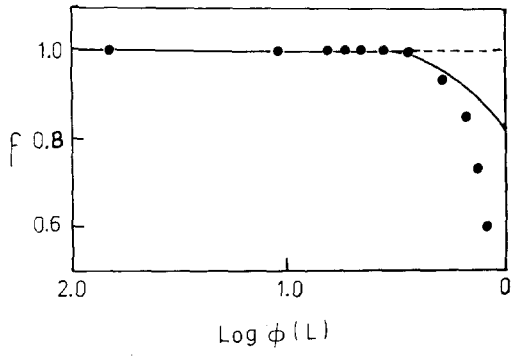

Fig. 4. Comparison of the theoretical and experimental efficiencies for the electrodeposition of Cu^{2+}.

values of f with theoretical predictions. The solid line was calculated for the values of $\theta q = 0{\cdot}47 \times 1{\cdot}75 = 0{\cdot}822$ obtained experimentally. The

agreement between theory and experiment is satisfactory for $\phi(L) < 0{\cdot}5$. Alternatively, the experimental limiting current is plotted versus flow speed on logarithmic scales in Fig. 5, for both oxygen reduction and copper deposition. The straight line portions with slopes of about unity correspond to Equation 9 when the exponential term is negligible, i.e. when radial diffusion is fast

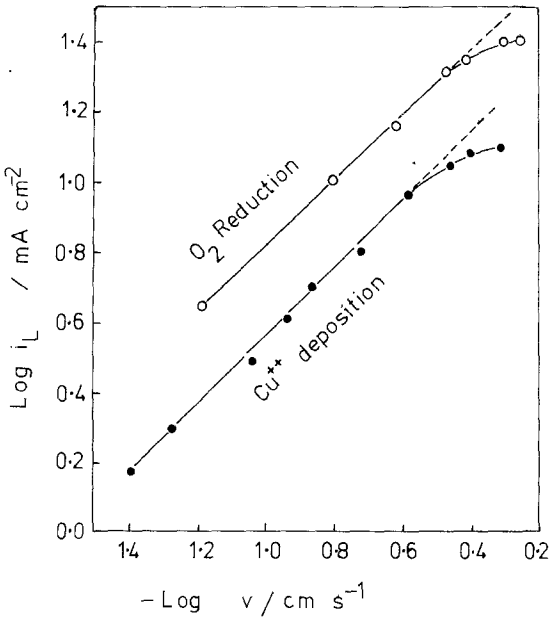

Fig. 5. Logarithmic plot of limiting current versus flow speed for reduction of oxygen and deposition of copper.

and hence 100% conversion is achieved. The curvature in the plots marks the onset of radial diffusion limitations on the limiting current. This occurs at $\phi(L) > 0{\cdot}5$. On analysing the results reported by Kenkel and Bard [5] for the electroreduction of Fe(III) on microporous electrodes, it was found that complete conversion was possible for $\phi(L) < 0{\cdot}6$ in agreement with the present results. This illustrates the general nature of the $\phi(L)$ criterion.

For $\phi(L) > 0{\cdot}5$, the experimental values of f become progressively less than those predicted by the model, indicating that radial diffusion limitations on f are actually greater than predicted. This can be explained on the basis that Equation 13 holds for fully developed profiles of velocity and of radial diffusion inside the electrode. For this condition to be fulfilled, the diffusional entrance length H must be negligible with respect to the electrode length. This is defined as the distance over which a steady radial diffusion profile is developing and is given by Levich [8] as $H \sim vr^2/D$. A closer approximation to this value is

$$H \simeq vr^2/2D. \tag{15}$$

For negligible diffusional entrance effects [6], $H/L = vr^2/2DL = \phi(L) < 0{\cdot}1$. Thus for $\phi(L) > 0{\cdot}5$ a steady radial diffusional profile is not established in more than one-half of the electrode length. For $\phi(L) > 1$, the entire length of the electrode is not sufficient for a steady radial diffusion profile to develop. In this diffusional entrance region a diffusional radial concentration profile is in the process of developing and neither Equation 1 nor 13 correctly predicts the electrode efficiency. The radial diffusional pattern in this region is similar to that in a tube where the limiting diffusion current is given by

$$i_{L3} = 2{\cdot}01nFDR_b(v^0x/Dr)^{1/3}r \tag{16}$$

where i_{L3} is the limiting diffusion current in a tube of radius r and x is the distance inside the tube. Equation 16 was derived by Levich [8] assuming that the diffusion layer thickness $\delta(x)$ is very small with respect to the pore radius. The value of $\delta(x)$ varies with distance and is given by

$$\delta(x) = (1/0{\cdot}67)(Drx/v^0)^{1/3}. \tag{17}$$

Hence $\delta(x)/r$ is

$$\delta(x)/r = (1/0{\cdot}67)[1/2\phi(x)]^{1/3}, \tag{18}$$

where $\phi(x) = vr^2/2Dx$ for Equation 16 to apply, $\delta(x)/r < 0{\cdot}1$ i.e. $\phi(x) > 1000$. This corresponds to large values of v and/or r and short distances e.g. in the velocity entrance length h. This velocity entrance length h is defined by Levich [8] as the distance beyond which a Poiseuille parabolic velocity profile is fully developed. This is given [6, 8] by

$$h \sim 0{\cdot}2vr^2/\nu \tag{19}$$

where ν is the kinematic viscosity. Consequently, there is a transition region where $0{\cdot}5 < \phi(x) < 1000$ which lies between the range of validity of Equations 1 and 16. In this transition region, it is obvious that i_{L2} is proportional to v^α where $0{\cdot}33 < \alpha < 1$, with the higher values of α corresponding to lower values of $\phi(L)$. The results of

Sioda [17], tabulated in reference [13] and of Alkire and Gracon [18], support these predictions. Thus for $\phi(L)$ values as large as 80, $\alpha = 0{\cdot}41$, whereas for lower values of $\phi(L)$, larger values of α were obtained.

5. Conclusions

On the basis of the above discussion, a porous flow-through electrode may be divided, in the most general case, into the following three regions, Fig. 6.

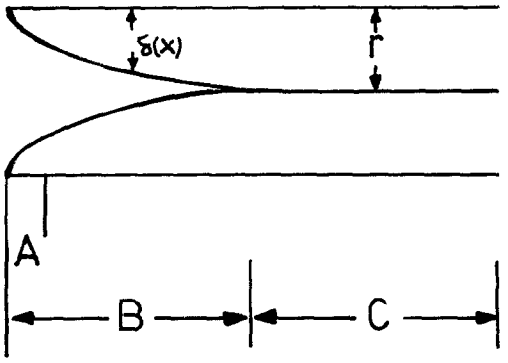

Fig. 6. Various regions in a porous flow-through electrode. $\phi(L) \simeq 0{\cdot}5$. Region A is highly exaggerated.

(1) Region A in which a parabolic velocity profile is developing. The length of this region is usually very short; $h \sim 0{\cdot}2vr^2/\nu$. Thus if $r = 10\,\mu$m, $\nu = 10^{-2}$ cm^2 s^{-1} and $v = 0{\cdot}1$ cm s^{-1}, then $h \sim 10^{-6}$ cm.

(2) Region B, the length of which $H \simeq vr^2/2D$. In this region a radial diffusional concentration profile is developing. Along this distance, the value of $\delta(x)$ increases from $\delta(x) \ll r$ at its beginning to $\delta(x) \simeq r$ at its end. Over the first part of this region, where $\delta(x) \ll r$ and $\phi(x) > 1000$, the limiting radial mass transfer flux is given by Equation 16. Region A is much shorter than B, $H/h \simeq 1000$, in view of the fact that $\nu/D = (Sc) \simeq 1000$ for normal aqueous solutions, where (Sc) is the Schmidt number. In both regions A and B, radial diffusion limits the conversion efficiency of the electrode.

(3) Region C starts at $\delta(x) \simeq r$ and $\phi(x) = 1$ and extends over the rest of the electrode where both velocity and radial diffusional concentration profiles are fully developed. In this region, radial diffusion does not limit the conversion efficiency and the limiting current obeys Equation 1.

References

[1] D. N. Bennion and J. Newman, *J. Appl. Electrochem.* **2** (1973) 113.
[2] A. K. P. Chu, M. Fleischmann and G. J. Hills, *ibid* **4** (1974) 323.
[3] A. T. Kuhn and R. W. Houghton, *ibid* **4** (1974) 69.
[4] G. B. Adams, R. P. Hollandswarth and D. N. Bennion, *J. Electrochem. Soc.* **122** (1975) 1043.
[5] J. A. Kenkel and A. J. Bard, *J. Electroanal. Chem.* **54** (1975) 47.
[6] B. G. Ateya, *J. Electroanal. Chem.* **76** (1977) 183.
[7] J. OM. Bockris and A. K. N. Reddy, 'Modern Electrochemistry', Vol. 1, Plenum, Rosetta (1973) p. 304.
[8] V. G. Levich, 'Physicochemical Hydrodynamics', Prentice Hall, Englewood Cliffs, N. J. (1962) pp. 113, 115.
[9] L. G. Austin, P. Palasi and R. Klimple, 'Advances in Chemistry Series', No. 47 (1965) p. 35.
[10] W. M. Rohsenow and H. Y. Choi, 'Heat, Mass and Momentum Transfer', Prentice Hall, Englewood Cliffs, N. J. (1961) p. 141.
[11] B. G. Ateya, 'Current-Polarisation Relations at Porous-Flooded Electrodes', Ph. D. Thesis, Pennsylvania State University (1972).
[12] L. G. Austin, in 'Handbook of Fuel Cell Technology', (Ed. C. Berger) Prentice Hall, Englewood Cliffs, N. J. (1968) p. 159, 161, 171.
[13] H. S. Wroblowa and G. Razumney, *J. Electroanal. Chem.* **49** (1974) 355.
[14] M. Muskat, 'The flow of homogeneous fluids through porous media', J. W. Edwards, Michigan (1946) p. 62.
[15] P. C. Carman, 'Flow of Gases Through Porous Media', Academic Press, New York (1956) p. 48.
[16] W. Eversole, H. Kindswater and J. Peterson, *J. J. Phys. Chem.* **46** (1942) 370.
[17] R. Sioda, *Electrochim. Acta* **13** (1968) 375, 1159; **15** (1970) 783.
[18] R. Alkire and B. Gracon, *J. Electrochem. Soc.* **122** (1975) 1594.